DMD Fast Forward. Published on September 22, 2006 as doi:10.1124/dmd.106.012351

Rapid Identification of P-glycoprotein Substrates and Inhibitors

Cheng Chang[1,2], *Praveen M. Bahadduri*[1], *James E. Polli, Peter W. Swaan and Sean Ekins*

Department of Pharmaceutical Sciences, University of Maryland, 20 Penn Street, Baltimore, MD 21201 (C.C., P.M.B, J.E.P, P.W.S. and S.E.) and ACT LLC, 601 Runnymede Avenue, Jenkintown, PA 19046 (S.E.)

Running title: Database mining for identifying P-gp Substrates and Inhibitors

Corresponding author: Peter W. Swaan, Ph.D., Department of Pharmaceutical Sciences, University of Maryland, Baltimore MD 21201. Tel. 410-706-0103. Email pswaan@rx.umaryland.edu

Number of Text pages:	39
Tables:	7
Figures:	3
References:	33
Words in Abstract:	204
Words in Introduction:	465
Words in Discussion:	1383

The abbreviations used are: BDDSC, biopharmaceutics drug disposition classification system; DDI, drug-drug interaction; P-gp, P-glycoprotein; QSAR, quantitative structure-activity relationship.

DMD Fast Forward. Published on September 22, 2006 as DOI: 10.1124/dmd.106.012351
This article has not been copyedited and formatted. The final version may differ from this version.

ABSTRACT

Identifying molecules that interact with P-glycoprotein (P-gp) is important for drug discovery but is also generally reliant on time consuming *in vitro* and *in vivo* studies. As an alternative approach, the current study applied pharmacophore models and database screening to rapidly retrieve molecules that bind as substrates or inhibitors for P-gp from commercial databases and then confirmed their affinity as inhibitors *in vitro*. Seven molecules (acitretin, cholecalciferol, misoprostol, nafcillin, repaglinide, salmeterol and telmisartan) with no published details for P-gp affinity, one positive control inhibitor (miconazole) and two negative control molecules (phenelzine and zonisamide) were selected for testing. The MDCK-MDR1 *in vitro* cell model was used to confirm their inhibitory effect on [^{3}H]-digoxin transport and the ATPase assay was used as an additional *in vitro* tool to indicate P-gp activation. All seven test drugs were confirmed to have P-gp affinity. Additionally, our experimental results provided plausible explanations for the published pharmacokinetic profiles of the tested drugs and their classification according to the biopharmaceutics and drug disposition classification system. In this study, we demonstrated the successful application of pharmacophore models to accurately predict P-gp binding, which holds promise to anticipate drug-drug interactions from screening drug databases and a priori prediction of novel P-gp inhibitors or substrates.

INTRODUCTION

Assessment of P-glycoprotein (P-gp, ABCB1) affinity in humans is a rate limiting step in the identification of drug efficacy and safety. Apart from serving as a key factor in the natural detoxification mechanism in various human tissues, expression of P-gp also mediates efflux of xenobiotics. This generally results in reduced bioavailability due to increased hepatic, renal and/or intestinal clearance of substrate drugs. Because of its frequent involvement in drug absorption, distribution, metabolism, and excretion (ADME), screening for *in vivo* and *in vitro* P-gp-mediated transport has become an essential component of the drug discovery process; this, in turn, may have led to the mounting costs of identifying clinical drug candidates. Attempts to co-administer P-gp modulators, inhibitors or inducers to increase cellular availability by blocking the actions of P-gp have been met with limited success. As a result, there is a great need to identify whether a new chemical entity has affinity for P-gp and to understand the effects of P-gp on drug pharmacokinetics and pharmacodynamics. Thus, the rapid identification of P-gp substrates or inhibitors would be advantageous.

Despite its overall significance, P-gp is poorly characterized at the atomic level in large part due to the intrinsic difficulties involved in membrane protein crystallization. As an alternative, computational modeling of transporters has aided our understanding and has significantly increased our knowledge of transporter mechanisms and drug-transporter interactions. However, in the case of P-gp, no single quantitative structure-activity relationships (QSAR) or pharmacophore model can describe the spatial arrangement of structural features responsible for substrate and inhibitor affinity (Stouch and Gudmundsson, 2002; Ekins and Swaan, 2004). This is reflected in the existence of

multiple models, which account for multiple binding sites and allosteric mechanisms of interaction. Thus, we have previously developed P-gp pharmacophore models from *in vitro* data for several cell systems using ***substrate*** transport data (Yates et al., 2003) as well as models with ***inhibition*** data (Ekins et al., 2002a; Ekins et al., 2002b).

In current drug discovery, the prospective application of pharmacophore models for database screening and the identification of P-gp substrates/inhibitors is limited (for a review, see (Chang and Swaan, 2005)) and not usually supported by experimental verification (Langer et al., 2004). Therefore, the objectives of the present study were to utilize and validate three unique P-gp pharmacophore models derived from substrate *and* inhibition data. These were applied to search structurally diverse molecular databases in order to identify molecules that bind to P-gp. Subsequently, a selection of retrieved compounds were tested *in vitro* to further validate and assess the predictive accuracy of the pharmacophore models. The successful identification of these novel molecules and demonstration of their *in vitro* activity, indicate that pharmacophore models for P-gp and other transporters are valuable tools for the efficient retrieval of novel or hitherto unrecognized molecules with binding affinity.

MATERIALS AND METHODS

***In silico* modeling: P-gp pharmacophore development with Catalyst™.** The molecular modeling studies were carried out on a Silicon Graphics (Palo Alto, CA) Octane workstation. Briefly, molecules described in the literature for P-gp were sketched in Catalyst™. The 3-D molecular structures were produced using up to 255 conformers with the BEST conformer generation method, allowing a maximum energy difference of 20kcal/mol. The three pharmacophore models were constructed using Catalyst™ version 4.9 (Accelrys, San Diego, CA). A previously published P-gp substrate HIPHOP model (Ekins et al., 2002b) based on verapamil and digoxin data was generated (Substrate Model). Since the substrate HIPHOP model is limited to identifying only large molecules a second model, the previously described P-gp digoxin inhibition HypoGen model (Ekins et al., 2002a) (Inhibitor Model 1) was also generated. To further update this latter model, 6 previously described test compounds with activity data were used (FK506A, PSC833, ritonavir, erythromycin, cyclosporine and CP99542) and incorporated into the training set (Ekins et al., 2002a) resulting in a second more comprehensive digoxin inhibition HypoGen model (Inhibitor Model 2) with 33 compounds. For each HypoGen model ten hypotheses were generated using hydrophobic, hydrogen bond acceptor, hydrogen bond donor, and the positive and negative ionizable features. After assessing all ten generated hypotheses, the hypothesis with lowest energy cost was selected for further analysis as this possessed features representative of all the hypotheses and had the lowest total cost.

The quality of the structure activity correlation between the estimated and observed activity values was estimated by means of an *r* value. The statistical significance of the Inhibitor model 2 was verified by permuting (randomizing) the

response variable ten times (so that each value was no longer assigned to the original molecule) and the Catalyst™ hypothesis generation procedure was repeated. The total energy cost of the generated pharmacophores was calculated from the deviation between the estimated activity and the observed activity, combined with the complexity of the hypothesis (i.e. the number of pharmacophore features). A null hypothesis which presumes that there is no relationship in the data and the experimental activities are normally distributed about their mean was also calculated. Hence, the greater the difference between the energy cost of the generated hypothesis and the energy cost of the null hypothesis, the less likely it is that the hypothesis reflects a chance correlation.

***In silico* modeling: Validation of the Catalyst models.** The various models were tested with molecules not included in the initial training sets derived from database searching described below. These test molecules were fit by the FAST-fit algorithm to the respective Catalyst™ models in order to predict a value as previously described for cytochrome P450s (Ekins et al., 1999). FAST fit refers to the method of finding the optimum fit of the substrate to the hypothesis among all the conformers of the molecule without performing an energy minimization.

***In silico* modeling: Database searches**. The three P-gp pharmacophore models were used to search different databases to provide a means of evaluation of their utility. Both databases were generated using structures in the MDL SDF format prior to conversion to a 3D Catalyst database after generating up to 100 molecule conformations with the FAST conformer generation method, allowing a maximum energy of 20 kcal/mol. The first database (P-gp Database) consisted of 189 known P-gp substrates and non-substrates (Penzotti et al., 2002) and was used to evaluate the performance of each

model as well as the different searching methods. Both the FAST (rigid) search method and BEST (flexible) search methods were applied to this database. The second in-house database (SCUT) consisted of 576 known drugs in clinical use in the USA derived from the Clinician's Pocket Drug Reference (Gomella and Haist, 2004). By screening this database, our pharmacophore models were put into a realistic situation to test their ability to identify previously unclassified drugs as possible P-gp substrates or inhibitors. The retrieved hits were used to search against PubMed (http://www.ncbi.nlm.nih.gov/entrez/query.fcgi) for previously documented P-gp affinity. Among the ones that have not been characterized before, seven were selected for further *in vitro* testing. One retrieved hit that has previously been documented as a P-gp inhibitor was also tested *in vitro* as a positive control. In addition, from the structures that did not fit the pharmacophores, two molecules were selected as negative controls for *in vitro* testing.

***In silico* modeling: Database analysis**. Database analysis assessment included the enrichment (*E*, Eq. 1) which indicates the ratio of yield of active compounds in the hit list relative to the yield of active compounds in the database.

$$E = \left(\frac{H_a / H_t}{A / D} \right) = \frac{H_a \times D}{H_t \times A} \qquad \text{(Eq. 1)}$$

where D is the total number of compounds in the database, A the number of active compounds in the database (e.g. substrates), H_t the number of compounds in a search hit list, and H_a the number of active compounds in the hit list. Secondly, the yield (*%Y*, Eq. 2) was determined which is the percentage of known active compounds in the hit list.

$$\%Y = \frac{H_a}{H_t} \times 100 \qquad \text{(Eq. 2)}$$

Thirdly, the coverage (*%A*, Eq. 3) was calculated which is the percentage of known active compounds retrieved from the database.

$$\%A = \frac{H_a}{A} \times 100 \qquad \text{(Eq. 3)}$$

Finally, the search effectiveness of each model from the P-gp database was evaluated using the Güner-Henry (GH) score (Guner and Henry, 2000) that is defined as:

$$GH = \left(\frac{H_a(3A + H_t)}{4H_t A} \right) \times \left(1 - \frac{H_t - H_a}{D - A} \right) \qquad \text{(Eq. 4)}$$

The GH score provides a combination of yield and coverage with a correction for the hit list size (Guner and Henry, 2000). Particularly, the correction is the ratio of the retrieved false positive hits over the inactive compounds in the database. Should the whole database be retrieved as a hit list, this correction will add a penalty as this is not reflected by either yield or coverage factor. Small but selective hit lists (high %Y but low %A) are very useful as this will represent fewer false positive hits. Therefore yield is more important than coverage and is given a weight of 0.75, while coverage has a weight of 0.25 in this formula (Eq. 4).

***In vitro* assays: Materials**. All chemicals and reagents used for the study were of the highest chemical purity available commercially. [^{3}H]-Digoxin (23.5Ci/mmol) was purchased from Perkin Elmer Life and Analytical sciences (Boston, MA). [^{14}C]-mannitol (53mCi/mmol) was purchased from Moravek Chemicals (Brea, CA). Digoxin, verapamil, acitretin, nafcillin, miconazole, misoprostal, salmeterol, telmisartan phenelzine and zonisamide were purchased from Sigma Chemical Company (St. Louis, MO).

Repaglinide was purchased from Toronto Research Chemicals, Toronto, Canada. Cholecalciferol was purchased from Supelco (Bellefonte, PA). GF120918 was a kind gift from GlaxoSmithKline, Research Triangle Park, NC. Hank's balanced salt solution (HBSS), Dulbecco's phosphate buffered saline (D-PBS), Dulbecco's modified eagle medium (DMEM), penicillin-streptomycin, fetal bovine serum (FBS), L-glutamine and non-essential amino acids (NEAA) were obtained from Gibco-Invitrogen corporation (Carlsbad, CA). Rat tail collagen Type I was purchased from Upstate (Waltham, MA). Cultureware and 12 well polycarbonate membrane Transwells® (0.4 μm pore size) were from Corning Costar (Corning, NY). P-gp expressing *Spodoptera frugiperda* (Sf9) membranes for P-gp ATPase activation assays were obtained from BD Biosciences (Bedford, MA).

***In vitro* assays: Cell culture**. MDCK strain II (MDCK-WT) epithelial cells and MDCK cells transfected with the human MDR1 gene (MDCK-MDR1) were gifts from Dr. Piet Borst (Netherlands Cancer Institute, Amsterdam, The Netherlands) and used within 10-20 passages from the original clone. MDCK-II and MDCK-MDR1 cells were maintained in DMEM with 10% FBS, 0.1mM NEAA, 2mM L-glutamine, 100U/ml penicillin and 100μg/ml streptomycin. Cells were split twice weekly at a dilution of 1:10. All cells were maintained at 37 °C in a humidified 5% CO_2 and 95% air atmosphere. The cells were used for transport assays after at least 3 passages upon removal from liquid nitrogen. It has been shown that the cells poorly express the P-gp protein during the initial phase of culturing probably due to the cells acclimatizing to the cell culture conditions (Polli et al., 2001). The cells were used within 2 months of culture. The

expression of the P-gp transporter in the transfected cells was assessed using Western blotting.

***In vitro* assays: Transport experiments**. The Transwells® were coated with 25 % rat tail collagen type I, before cell seeding at a density of 50,000 cells/cm^2. Media for the cells was changed every 2 days and experiments were conducted after 3-6 days in culture. The development of tight junctions was monitored by assessing transepithelial electrical resistance (TEER), using the Endohm meter (World Precision Instruments, Sarasota, FL). Inserts with TEER values < 250Ω.cm^2 were discarded. Putative inhibitors were dissolved in 100% DMSO or ethanol or methanol or buffer depending on their solubility and were prepared fresh before each study. Further dilutions (3% final solvent concentration) were prepared in the transport buffer, HBSS with 10mM HEPES (pH 7.4). Bidirectional transport of 0.05μM [^{3}H]-digoxin was monitored in the presence of compounds at 100-fold excess (5 μM) concentrations. The paracellular marker [^{14}C]-mannitol (2.9 μM) was used in all test solutions to confirm the formation of functional tight junctions. The inserts were given two quick washes with transport buffer and incubated with drug solutions for 30min at 37°C. Bidirectional transport assays were performed by replacing solutions on the acceptor and donor sides with [^{3}H]-digoxin and [^{14}C]-mannitol prepared in the test drug solution. For control studies, only [^{3}H]-digoxin and [^{14}C]-mannitol were added to the acceptor and donor chambers. MDCK-II cells were used as control, cultured and seeded similarly. 50μl samples were withdrawn every 30, 60, 90, 120, 150 and 180 min intervals. Sink conditions were maintained after aliquots were taken from the respective chambers during the transport studies. The apparent permeability was calculated using the steady-state rate constant (Eq. 5):

DMD Fast Forward. Published on September 22, 2006 as DOI: 10.1124/dmd.106.012351
This article has not been copyedited and formatted. The final version may differ from this version.

$$P_{app} = J \big/ A \cdot C_0 \qquad \text{(Eq. 5)}$$

Where, P_{app} is the apparent permeability (cm/s), J the solute flux (dpm/min), A the effective growth area (cm^2) and C_0 the initial dosing concentration (dpm/ml). The net efflux was calculated from Eq. 6

$$ER = \frac{P_{app(B \to A)}}{P_{app(A \to B)}} \qquad \text{(Eq. 6)}$$

Where, ER is efflux ratio, $P_{app(B \to A)}$ is P_{app} in B→A direction and $P_{app(A \to B)}$ is P_{app} in A→B direction. The experiments were performed in triplicate and represent three separate determinations (n = 3).

***In vitro* assays: ATPase activation assay**. Using P-gp expressing Sf9 membranes the inorganic phosphate released from ATP as a result of drug-stimulated P-gp ATPase activity was estimated as mentioned in the manufacturer's protocol. All compounds were tested at a concentration of 20μM. Verapamil (20μM) was used as a positive control. The concentration range was selected based on previous published reports that demonstrated that this concentration would provide adequate ATPase activation for the majority of compounds (Litman et al., 1997; Polli et al., 2001). Briefly, membranes (30μg per well) prepared in Tris-MES buffer, pH 6.8 (50mM Tris-MES, pH 6.8, 50mM KCl, 5mM sodium azide, 2mM EGTA, 2mM DL-dithiothreitol) were incubated at 37 °C on a 96 well-plate for 5 min with test compounds in the presence or absence of 300μM sodium orthovanadate (in duplicate). The reaction was initiated by the addition of 12mM Mg-ATP (20μl), and after 20min incubation, terminated by addition of 10% SDS containing antifoam A (30μl). The inorganic phosphate released was detected by incubation at 37 °C for 20 min with 200μl detection reagent (1:4 v/v mixture of 35mM ammonium molybdate

in 15mM zinc acetate (pH 5.0) and 10% ascorbic acid). Phosphate standards were prepared in each plate. The absorbance was measured at 800nm using a Spectramax Gemini UV-VIS spectrophotometer (Molecular. Devices, Sunnyvale, CA). The drug stimulated ATPase activity (nmol/min/mg of protein) was determined as the difference between the amounts of inorganic phosphate released from ATP in the absence and presence of vanadate. The drug-stimulated P-gp ATPase activity was reported as fold-stimulation relative to the basal P-gp ATPase activity in the absence of drug (DMSO control).

***In vitro* assays: Western blotting and protein detection**. MDCK-II and MDCK-MDR1 cell lysates for cells from each passage used for transport studies were prepared according to the standard protocol and the protein concentration was determined using the Bio-Rad protein assay kit (Bradford method, Bio-Rad, Hercules, CA). A uniform concentration of protein was resolved on a 7.5% Tris-HCl gel and transferred onto a PVDF membrane. The blot was processed for anti-P-gp (1:1000) and anti β-tubulin antibody (1:1000) (Santa Cruz Biotechnology, Santa Cruz, CA) after blocking overnight with 5% not-fat dry milk prepared in D-PBS (pH 7.4) with 0.1 % Tween-20. After washing the blot was incubated with a horseradish peroxidase-conjugated secondary antibody. The immnuoreactive blots after washes were visualized using the enhanced chemiluminescence plus (ECL+) detection system (Amersham Pharmacia,UK). P-gp expression levels were validated over the period in which transport studies were performed and were found to be largely consistent across the cell passages (data not shown).

DMD Fast Forward. Published on September 22, 2006 as DOI: 10.1124/dmd.106.012351
This article has not been copyedited and formatted. The final version may differ from this version.

RESULTS

***In silico* modeling.** In the present study two pharmacophores for P-gp inhibitors and substrates (Inhibitor model 1 and the P-gp substrate model, respectively) were evaluated (Ekins et al., 2002a; Ekins et al., 2002b). A third, unique Catalyst P-gp pharmacophore model (Inhibitor model 2) was developed with the 33 molecules (activity range 0.024 – 100 μM) and consisted of 4 hydrophobic (HYD) features and 1 hydrogen bond acceptor (HBA) features (Table 3). The observed versus predicted IC_{50} data revealed a linear correlation with an *r* value of 0.87 and acceptable model statistics (Kristam et al., 2005) (Table 4). Following randomization, the average training correlation decreases to 0.56 and the difference between the total cost (model) and null cost narrowed considerably (Table 4), indicative of a significant model (Kristam et al., 2005).

All three pharmacophores were then used to search molecular databases. For the P-gp database, the results were analyzed using several metrics (defined in *Materials and Methods*) (Guner and Henry, 2000) and are listed in Table 5. Due to the wider coverage of the BEST search algorithm, more true positive hits (i.e. known P-gp substrates or inhibitors) were retrieved when compared to the FAST search algorithm (Table 5). Simultaneously, a high number of false positive hits were also returned. This resulted in generally lower GH scores when compared with the FAST search algorithm. This result echoes the previous observations by Guner and colleagues for other types of pharmacophores and databases (Guner and Henry, 2000). Overall, in this study the GH scores for the P-gp database indicated the usefulness of the less computationally intensive FAST search approach over the BEST search algorithm, resulting in lower computational

overhead. The P-gp substrate pharmacophore model had relatively higher GH scores compared to the two inhibition models, likely due to its improved enrichment and yield factors.

As the various P-gp pharmacophores may retrieve identical molecules, we analyzed the molecules identified by visualizing their overlap using Venn diagrams (Fig. 1a). A high degree of overlap is observed between the inhibitor models, while the substrate model identifies a smaller subset of molecules shared between all three models. The average molecular properties of each set of retrieved hits also indicate that the more stringent substrate model retrieved molecules characterized by a significantly higher average number of hydrogen-bond acceptors and donors, as well as a higher average molecular weight (Table 6). In contrast, the compounds retrieved by inhibitor models 1 and 2 have similar values for these molecular properties. Interestingly, compounds retrieved by all three models have nearly equal molecular flexibility as represented by the total number of rotatable bonds. These data effectively validate the three independent pharmacophore models. Their efficacy was further determined using the in-house SCUT database of compounds with unknown P-gp affinity. All of the retrieved molecules from database searching were subjected to a thorough literature analysis to determine their prior experimental confirmation as a P-gp substrate. 40 drugs were retrieved by Inhibitor model 1, of which 25 were known P-gp substrates or inhibitors. For Inhibitor model 2, 68 drugs were retrieved containing 34 verified P-gp substrates or inhibitors. For the substrate model, 4 out of the 6 returned drugs were known P-gp substrates or inhibitors (Figure 1b). *Importantly, of the remaining hits identified by the various models, there are no data available to definitively verify their status as P-gp* substrates or inhibitors. *Therefore, the*

number of actual positive hits identified by these models could be much greater than stated here. Thus, as the number of experimentally verified P-gp substrates or inhibitors within the database was unknown, we were unable to perform statistical analysis on the search results from the SCUT database.

Among the remaining drugs with no reported P-gp affinity, we selected seven for *in vitro* testing based on their mapping to the pharmacophore as well as their commercial availability. As a positive control, a known P-gp inhibitor (miconazole) that was also retrieved by the pharmacophore was selected for *in vitro* testing. For comparison, the eight putative P-gp substrates or inhibitors and the model substrate CP114416 were mapped to Inhibitor model 2 pharmacophore (Fig. 2). To test their robustness, the other two pharmacophores were used to score the selected molecules (Table 1) and two additional positive controls (verapamil and the selective P-gp inhibitor LY335979). The FAST fit of verapamil to the substrate pharmacophore has a score of 4.54 and LY335979 has a score of 3.29 and 5.72 to Inhibitor model 1 and Inhibitor model 2, respectively. The pharmacophore fit scores and predicted IC_{50} values for the molecules selected for experimental verification are similar to the standard substrate and inhibitor molecules. The two negative controls retrieved from the SCUT database (phenelzine, zonisamide) did not fit any of the models (Table 1).

***In vitro* assays**. The selected compounds were tested for inhibition of [^{3}H]-digoxin transport in the MDCK-MDR1 cell monolayer model. Control and verapamil-treated BL-AP and AP-BL P_{app} values were compared to determine the contribution of verapamil-sensitive efflux for the model substrate, digoxin. The efflux ratio for [^{3}H]

digoxin was approximately 15.2, which is comparable to studies by Taub and colleagues (Taub et al., 2005) who reported a [^{3}H] digoxin (at 20nM) efflux ratio of 25.5. The apparent permeability coefficient (P_{app}) of [^{14}C]-mannitol across MDCK-II and MDCK-MDR1 monolayers was typically in the range of 4.0-7.0x10^{-6} cm/s, in line with other studies (Tang et al., 2002). TEER values were measured at the start and at the end of each transport experiment and were typically between the acceptable range of 700-800 $\Omega \cdot cm^2$. The decrease in TEER values over the course of an experiment was generally less than 10%, indicating the preservation of monolayer integrity. The efflux ratio of [^{3}H]-digoxin in MDCK-II cell and MDCK-MDR1 monolayers (Table 2) was within previously reported values (Tang et al., 2002). As expected, complete inhibition of P-gp-mediated [^{3}H]-digoxin efflux was observed in the presence of verapamil (25 μM) and GF120918 (2.0 μM) in MDCK-II as well as MDCK-MDR1 cell monolayers, which is comparable to studies by other groups (Polli et al., 2001; Tang et al., 2002). All other compounds tested showed potent inhibitory activity (Table 2), except for the two negative controls, zonisamide and phenelzine. Misoprostol was excluded from the data table due to unacceptably high [^{14}C]-mannitol P_{app}(B to A). All compounds were further characterized using the ATPase activation assay (Schmid et al., 1999). Verapamil strongly stimulates the P-gp-mediated ATPase activity as compared to the other tested compounds (Figure 3), yet the negative controls, zonisamide and phenelzine do not. Amongst the tested compounds, a greater than two-fold increase in ATPase activity was observed for nafcillin and miconazole, misoprostol, telmisartan suggesting that these compounds are also likely P-gp substrates.

DISCUSSION

The need for predictive models.

The application of pharmacophore modeling to determine substrate or inhibitor specificity has greatly advanced our mechanistic understanding of drug transporters (Chang and Swaan, 2005). To date, several P-gp models derived from both efflux and inhibition data have been reported (Ekins and Swaan, 2004; Chang and Swaan, 2005), but application of these models to identify novel P-gp substrates or inhibitors has not been explored. Recently, Langer and colleagues (Langer et al., 2004) described a P-gp pharmacophore that was subsequently utilized to screen molecular databases to select putative P-gp inhibitors. However, without *in vitro* validation of the predicted molecules, the impact of the work and the validity of the predictions remains to be demonstrated.

To overcome limitations of previous studies, our present work applied three distinct P-gp pharmacophore models in database screening studies using the GH score as a metric for assessing the efficacy of the respective pharmacophore models (Guner and Henry, 2000). Specifically, the implementation of the GH score here can be used as a determinant of the effectiveness of the model in retrieving true and false positives from the database using standard search algorithms. Thus, the resulting hit lists simultaneously served as a means of model validation and assisted in the selection of molecules for subsequent *in vitro* testing. GH scores indicated that all three computational pharmacophore models, particularly the P-gp *substrate* model, were able to significantly enrich and successfully identify P-gp substrates from non-substrates (Table 5). Additionally, the two *inhibitor* pharmacophores were capable of retrieving a considerable

number of validated P-gp substrates or inhibitors.

Newly Identified substrates or inhibitors

To further test whether our models could successfully identify known P-gp substrates or inhibitors as well as predict novel substrates or inhibitors, the pharmacophore models were used to screen an in-house database of nearly 600 frequently prescribed drugs (SCUT). The hit list of retrieved molecules contained ~50% confirmed P-gp substrates or inhibitors; from the remaining molecules, which had no reported P-gp affinity in the literature and were commercially available, we selected seven high-scoring molecules for *in vitro* testing (Fig. 2). Using a [^{3}H]-digoxin efflux assay, we confirmed that all selected compounds were P-gp inhibitors, except for misoprostol (Table 2). which may have been caused by cellular cytotoxicity at the concentrations studied. However, misoprostol showed strong activation of ATPase (Fig. 3) suggesting its P-gp affinity. The positive control, miconazole, is an established P-gp inhibitor (Yasuda et al., 2002; Schwab et al., 2003) and was successfully identified by both *in silico* and *in vitro* experiments. Two negative controls (phenelzine and zonisamide) did not significantly inhibit [^{3}H]-digoxin efflux or induce ATPase activation. Although there are no published interactions between any of these molecules and P-gp, there are several examples of drugs within the same therapeutic class and similar molecular structure with reported affinity for P-gp. For example, calciferol is structurally similar to cholecalciferol (differing by only a double bond and a methyl group) and was shown to inhibit P-gp in yeast (Saeki et al., 1991). Similarly, dicloxacillin, which falls in the same therapeutic class as nafcillin (β-lactam antibiotics) has been identified as a potent P-gp inhibitor (Susanto and Benet, 2002). Salmeterol, structurally related to the β2-adrenergic receptor

agonist salbutamol, is a known P-gp inhibitor (Valenzuela et al., 2001). Although purported P-gp activity based on structural associations is speculative in nature, it may serve as a suggestive indication of potential P-gp interactions for a given therapeutic class that may warrant further testing. For example, acitretin belongs to the retinoid family and although there is strong evidence of P-gp induction by retinoic acid (Kizaki et al., 1996) and retinol (Frota et al., 2004), there is no direct evidence for P-gp interaction. Thus, our study provides the first direct evidence of retinoid affinity for P-gp. These *in vitro* evaluations represent preliminary studies that confirmed the inhibitory role of each tested compound. More quantitative and definitive future experiments are warranted to fully characterize the interaction of each individual compound with P-gp as substrates.

Clinical Pharmacokinetic Implications

The biopharmaceutics classification system (BCS) has been used as a helpful guide to classify compounds based on their aqueous solubility and gastrointestinal permeability (Amidon et al., 1995). Wu and Benet (Wu and Benet, 2005) recently recognized that the clinical impact of efflux transporters in modulating oral absorption and drug pharmacokinetics is reserved to class 2 and possibly class 4 compounds. For example, high permeability allows facile cellular penetration for class 2 compounds, but low solubility (perhaps mainly due to high lipophilicity) will limit the effective concentration entering the cell, thereby preventing saturation of efflux transporters. Consequently, efflux transport can affect class 2 compounds' extent of oral bioavailability and their rate of absorption (Wu and Benet, 2005). Thus, classification of compounds according to BDDCS (Biopharmaceutics Drug Disposition Classification System) guidelines may allow for a scientific basis towards their observed clinical

behavior as a result of their interactions with P-gp. This, in turn, allows for a further understanding of their pharmacokinetic behavior and their potential for drug-drug interactions (DDI). Thus, we expect the compounds identified in this study as P-gp substrates or inhibitors to primarily belong to BDDCS classes 2 and 4.

Classifications were based on various parameters including physicochemical properties (cLogP and aqueous solubility), metabolism, bioavailability and food effects (Table 7). Misoprostol and verapamil are both *Class 1* compounds based on their high membrane permeability and high solubility characteristics. Miconazole, acitretin, cholecalciferol, repaglinide, and salmeterol can be classified as *Class 2* drugs based on the following observations: Miconazole displays high permeability (rapidly absorbed) and low bioavailability (~30%), undergoing extensive metabolism with less than 1% of the administered dose excreted in the urine unchanged (Stevens, 1983); Oral bioavailability of acitretin, cholecalciferol and repaglinide is 56-60%; Oral absorption of acitretin increases when administered with food (Wiegand and Chou, 1998); Cholecalciferol and salmeterol are extensively metabolized and readily absorbed; Clinical studies indicate that known P-gp substrates such as phenobarbital (Wikinski, 2005) and phenytoin (Bialecka et al., 2005) reduce plasma levels of vitamin D, suggesting a possible P-gp-mediated DDI involving cholecalciferol; A DDI was recently observed during the co-administration of repaglinide with the known P-gp inhibitor cyclosporine A, which markedly raises the plasma concentrations of repaglinide in humans (Kajosaari et al., 2005). Based on our current studies and these clinical observations, we can deduce that the affinity of repaglinide for P-gp significantly contributes to potential DDI with other P-gp substrates or inhibitors. Nafcillin, on the other hand, though soluble in

aqueous media, is poorly metabolized thereby justifying its *Class 3* categorization (Nahata et al., 1990). To our best knowledge, no reported DDI have been recorded for this drug. Telmisartan is insoluble in aqueous media and is eliminated unchanged (98%) via the biliary route (Stangier et al., 2000), thus categorizing it as *Class 4*. Furthermore, administration of telmisartan in multiple doses with the known P-gp substrate digoxin results in significantly higher serum digoxin concentrations (Stangier et al., 2000). This strongly indicates competition between telmisartan and digoxin with P-gp. Comparison of BDDCS classification and P-gp results indicate that Class 2 and 4 compounds showed clinical evidence of P-gp-mediated DDI, whereas predicted P-gp substrates or inhibitors in Classes 1 and 3 did not. This observation further supports claims by Wu and Benet that Class 2 and 4 drugs are more susceptible to the effects of efflux transporters (Wu and Benet, 2005).

In conclusion, the pharmacophore-based screening approach outlined in this study using different databases could represent a method to either filter out P-gp substrates or inhibitors *a priori* and identify potential therapeutic P-gp inhibitors. This would be particularly useful to avoid compounds with a potential P-gp interaction or efficiently select molecules to be screened *in vitro* in lead identification for drug discovery programs. We have demonstrated in this study that pharmacophore models generated with limited numbers of substrates or inhibitors can be used to efficiently identify other confirmed substrates or inhibitors that were not included in the model, as well as suggest new potential molecules for testing. Finally, we showed that classification of these compounds according to the BCCDS can provide a rational basis for their observed clinical actions. Thus, the combination of an iterative *in silico* and *in vitro* approach

represents a means to rapidly identify and subsequently validate molecules as substrates or inhibitors for a protein of interest.

ACKNOWLEDGMENTS

We gratefully acknowledge the considerable efforts of Mr. John Ohrn (Accelrys, San Diego, CA) for making Catalyst available to us. We also thank Dr. Osman Güner for suggestions relating to the implementation of the GH score.

REFERENCES

Amidon GL, Lennernas H, Shah VP and Crison JR (1995) A theoretical basis for a biopharmaceutic drug classification: the correlation of in vitro drug product dissolution and in vivo bioavailability. *Pharm Res* **12:**413-420.

Bialecka M, Hnatyszyn G, Bielicka-Cymerman J and Drozdzik M (2005) [The effect of MDR1 gene polymorphism in the pathogenesis and the treatment of drug-resistant epilepsy]. *Neurol Neurochir Pol* **39:**476-481.

Chang C and Swaan PW (2005) Computational approaches to modeling drug transporters. *Eur J Pharm Sci* **27:**411-424.

Ekins S, Bravi G, Binkley S, Gillespie JS, Ring BJ, Wikel JH and Wrighton SA (1999) Three and four dimensional-quantitative structure activity relationship analyses of CYP3A4 inhibitors. *J Pharm Exp Ther* **290:**429-438.

Ekins S, Kim RB, Leake BF, Dantzig AH, Schuetz E, Lan LB, Yasuda K, Shepard RL, Winter MA, Schuetz JD, Wikel JH and Wrighton SA (2002a) Application of three dimensional quantitative structure-activity relationships of P-glycoprotein inhibitors and substrates. *Mol Pharmacol* **61:**974-981.

Ekins S, Kim RB, Leake BF, Dantzig AH, Schuetz E, Lan LB, Yasuda K, Shepard RL, Winter MA, Schuetz JD, Wikel JH and Wrighton SA (2002b) Three dimensional quantitative structure-activity relationships of inhibitors of P-glycoprotein. *Mol Pharmacol* **61:**964-973.

Ekins S and Swaan PW (2004) Development of computational models for enzymes, transporters, channels and receptors relevant to ADME/TOX. *Rev Comp Chem* **20:**333-415.

Frota ML, Jr., Klamt F, Dal-Pizzol F, Schiengold M and Moreira JC (2004) Retinol-induced mdr1 and mdr3 modulation in cultured rat Sertoli cells is attenuated by free radical scavengers. *Redox Rep* **9:**161-165.

Gomella L and Haist S (2004) *Clinician's pocket drug reference 2004*. McGraw-Hill.

Guner OF and Henry DR (2000) Metric for analyzing hit lists and pharmacophores, in: *Pharmacophore perception, development, and use in drug design* (Guner OF ed), pp 191-211, International University Line, La Jolla, CA.

Kajosaari LI, Niemi M, Neuvonen M, Laitila J, Neuvonen PJ and Backman JT (2005) Cyclosporine markedly raises the plasma concentrations of repaglinide. *Clin Pharmacol Ther* **78:**388-399.

Kizaki M, Ueno H, Yamazoe Y, Shimada M, Takayama N, Muto A, Matsushita H, Nakajima H, Morikawa M, Koeffler HP and Ikeda Y (1996) Mechanisms of retinoid resistance in leukemic cells: possible role of cytochrome P450 and P-glycoprotein. *Blood* **87:**725-733.

Langer T, Eder M, Hoffmann RD, Chiba P and Ecker GF (2004) Lead identification for modulators of multidrug resistance based on in silico screening with a pharmacophoric feature model. *Arch Pharm (Weinheim)* **337:**317-327.

Litman T, Zeuthen T, Skovsgaard T and Stein WD (1997) Competitive, non-competitive and cooperative interactions between substrates of P-glycoprotein as measured by its ATPase activity. *Biochim Biophys Acta* **1361:**169-176.

Nahata MC, Fan-Havard P, Kosnik EJ, Bartkowski MH and Barson WJ (1990) Pharmacokinetics and cerebrospinal fluid concentration of nafcillin in pediatric patients undergoing cerebrospinal fluid shunt placement. *Chemotherapy* **36:**98-102.

Penzotti JE, Lamb ML, Evenson E and Grootenhuis PDJ (2002) A computational ensemble pharmacophore model for identifying substrates of P-glycoprotein. *J Med Chem* **45:**1737-1740.

Polli JW, Wring SA, Humphreys JE, Huang L, Morgan JB, Webster LO and Serabjit-Singh CS (2001) Rational use of in vitro P-glycoprotein assays in drug discovery. *J Pharmacol Exp Ther* **299:**620-628.

Saeki T, Shimabuku AM, Azuma Y, Shibano Y, Komano T and Ueda K (1991) Expression of human P-glycoprotein in yeast cells--effects of membrane component sterols on the activity of P-glycoprotein. *Agric Biol Chem* **55:**1859-1865.

Schmid D, Ecker G, Kopp S, Hitzler M and Chiba P (1999) Structure-activity relationship studies of propafenone analogs based on P-glycoprotein ATPase activity measurements. *Biochem Pharmacol* **58:**1447-1456.

Schwab D, Fischer H, Tabatabaei A, Poli S and Huwyler J (2003) Comparison of in vitro

P-glycoprotein screening assays: recommendations for their use in drug discovery. *J Med Chem* **46:**1716-1725.

Stangier J, Schmid J, Turck D, Switek H, Verhagen A, Peeters PA, van Marle SP, Tamminga WJ, Sollie FA and Jonkman JH (2000) Absorption, metabolism, and excretion of intravenously and orally administered [14C]telmisartan in healthy volunteers. *J Clin Pharmacol* **40:**1312-1322.

Stevens DA (1983) Miconazole in the treatment of coccidioidomycosis. *Drugs* **26:**347-354.

Stouch TR and Gudmundsson O (2002) Progress in understanding the structure-activity relationships of P-glycoprotein. *Adv Drug Del Rev* **54:**315-328.

Susanto M and Benet LZ (2002) Can the enhanced renal clearance of antibiotics in cystic fibrosis patients be explained by P-glycoprotein transport? *Pharm Res* **19:**457-462.

Tang C, Lin Y, Rodrigues AD and Lin JH (2002) Effect of albumin on phenytoin and tolbutamide metabolism in human liver microsomes: an impact more than protein binding. *Drug Metab Dispos* **30:**648-654.

Taub ME, Podila L, Ely D and Almeida I (2005) Functional assessment of multiple P-glycoprotein (P-gp) probe substrates: influence of cell line and modulator concentration on P-gp activity. *Drug Metab Dispos* **33:**1679-1687.

Valenzuela B, Nacher A, Casabo VG and Martin-Villodre A (2001) The influence of

active secretion processes on intestinal absorption of salbutamol in the rat. *Eur J Pharm Biopharm* **52:**31-37.

Wiegand UW and Chou RC (1998) Pharmacokinetics of acitretin and etretinate. *J Am Acad Dermatol* **39:**S25-33.

Wikinski S (2005) [Pharmacokinetic mechanisms underlying resistance in psychopharmacological treatment. The role of P-glycoprotein]. *Vertex* **16:**438-441.

Wishart DS, Knox C, Guo AC, Shrivastava S, Hassanali M, Stothard P, Chang Z and Woolsey J (2006) DrugBank: a comprehensive resource for in silico drug discovery and exploration. *Nucleic Acids Res* **34:**D668-672.

Wu CY and Benet LZ (2005) Predicting drug disposition via application of BCS: transport/absorption/ elimination interplay and development of a biopharmaceutics drug disposition classification system. *Pharm Res* **22:**11-23.

Yasuda K, Lan L-B, Sanglard D, Furoya K, Schuetz JD and Schuetz EG (2002) Interaction of cytochrome P450 3A inhibitors with P-glycoprotein. *J Pharm Exp Thera* **303:**323-332.

Yates CR, Chang C, Kearbey JD, Yasuda K, Schuetz EG, Miller DD, Dalton JT and Swaan PW (2003) Structural determinants of P-glycoprotein-mediated transport of glucocorticoids. *Pharm Res* **20:**1794-1803.

FOOTNOTES PAGE

a) Unnumbered Footnote:

This work was supported in part by the National Institutes of Health, grant DK61425 (to P.W.S.).

b) Send reprint requests to:

Peter W. Swaan, Ph.D., Department of Pharmaceutical Sciences, University of Maryland, Baltimore MD 21201. Tel. 410-706-0103. Email pswaan@rx.umaryland.edu

c) Numbered footnotes

[1]C.C and P.B. contributed equally to this work and should be considered co-first authors.

[2]Present address: Pfizer, Inc., 2800 Plymouth Road, Ann Arbor, MI 48105

DMD Fast Forward. Published on September 22, 2006 as DOI: 10.1124/dmd.106.012351
This article has not been copyedited and formatted. The final version may differ from this version.

FIGURE LEGENDS

Figure 1. Venn diagrams visualizing overlap of known P-gp substrates retrieved from the P-gp database (**a**) and the SCUT database (**b**) following searches using the three pharmacophore models.

Figure 2 a. Pharmacophore model for inhibitor model 2 aligned with CP114416. Green spheres indicate hydrogen bonding acceptor (HBA) features and cyan spheres indicate hydrophobic (HYD) features. **b.** Molecules selected with the Inhibitor model 2 for *in vitro* testing aligned with inhibitor model 2.

Figure 3. ATPase activation assay. P-gp expressing Sf9 membranes were used to assess the inorganic phosphate released from ATP as a result of drug-stimulated P-gp ATPase activity. All compounds were tested at a concentration of 20μM. Verapamil was used as a positive control. The drug-stimulated ATPase activity (nmol/min/mg of protein) was determined as the difference between the amounts of inorganic phosphate released from ATP in the absence and presence of vanadate and reported as fold-stimulation relative to the basal P-gp ATPase activity in the absence of drug (DMSO control).

DMD Fast Forward. Published on September 22, 2006 as DOI: 10.1124/dmd.106.012351
This article has not been copyedited and formatted. The final version may differ from this version.

Table 1. Molecules predicted following SCUT database search with Inhibitor Models 1 and 2

		Inhibitor model 1		Inhibitor model 2		
Name	Structure	Fit	predicted IC_{50}	Fit	predicted IC_{50}	Substrate model fit
Acitretin	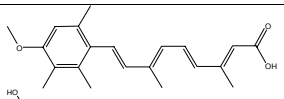	2.59	7.5	6.68	2.5	3.63
Cholecalciferol	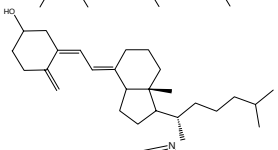	2.52	8.8	6.34	5.5	NF
Miconazole	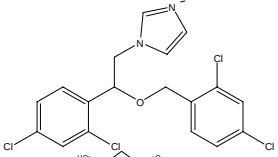	2.61	7.1	6.66	2.7	NF
Misoprostol	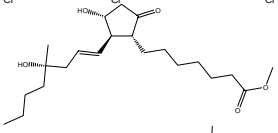	2.64	6.7	6.83	1.8	3.06
Nafcillin	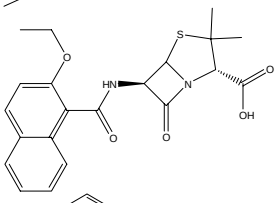	2.52	8.9	6.98	1.3	NF
Repaglinide	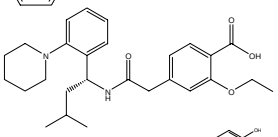	2.67	6.2	5.79	20	1.35
Salmeterol	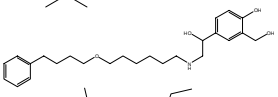	2.62	6.9	6.51	3.7	3.87
Telmisartan	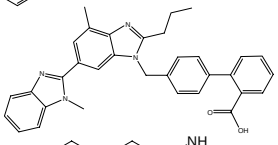	2.88	3.9	7.02	1.2	3.81
Phenelzine	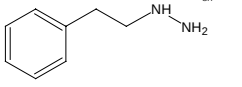	NF[a]	NF	NF	NF	NF
Zonisamide	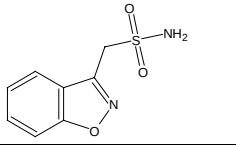	NF	NF	NF	NF	NF

[a]NF= does not fit to pharmacophore

DMD Fast Forward. Published on September 22, 2006 as DOI: 10.1124/dmd.106.012351
This article has not been copyedited and formatted. The final version may differ from this version.

Table 2. AP-BL and BL-AP P_{app} and efflux ration of [^{3}H] digoxin across MDCK-II and MDCK-MDR1 monolayers in the presence and absence of various inhibitors

	[^{3}H] Digoxin (50 nM) efflux assay (P_{app}± SDx10^{-06} cm/s)[a]		
	P_{app}(A to B)	P_{app}(B to A)	Efflux ratio
	MDCK-II control		
[^{3}H] Digoxin alone	2.52±0.83	8.74±2.30	3.46
[^{3}H] Digoxin with:			
GF120918 (2μM)	5.02±0.046	5.21±0.047	1.04
Verapamil (25μM)	3.40±0.30	4.29±0.33	1.26
	MDCK-MDR1[b]		
[^{3}H] Digoxin alone	0.99±0.11	15.2±3.42	15.2
[^{3}H] Digoxin with:			
GF120918 (2.0 μM)	2.09±0.42	2.04±0.59	0.98
Verapamil (25 μM)	1.81±0.56	3.96±0.49	2.11
Repaglinide	3.37±1.36	5.00±1.85	1.48
Acitretin	3.31±1.50	6.51±1.73	1.97
Cholecalciferol	3.53±1.26	7.12±2.14	2.02
Telmisartan	2.92±1.36	6.54±2.01	2.24
Miconazole	2.80±1.46	7.22±1.29	2.58
Nafcillin	2.23±1.41	7.08±2.60	3.18
Salmeterol	1.63±0.58	11.1±1.37	6.81

DMD Fast Forward. Published on September 22, 2006 as DOI: 10.1124/dmd.106.012351
This article has not been copyedited and formatted. The final version may differ from this version.

Misoprostal	N/A	N/A	N/A
Phenelzine	0.55±0.09	9.13±0.29	16.61
Zonisamide	0.53±0.08	10.1±1.13	18.77

Notes: [a]n = 6; [b] all compounds were tested at 5μM unless otherwise noted; N/A: Not available;

DMD Fast Forward. Published on September 22, 2006 as DOI: 10.1124/dmd.106.012351
This article has not been copyedited and formatted. The final version may differ from this version.

Table 3. Cartesian coordinates for inhibitor pharmacophore 2.

Feature		[a]HBA		[b]HYD	HYD	HYD	HYD
Weight		1.93		1.93	1.93	1.93	1.93
Tolerance		1.60	2.20	1.60	1.60	1.60	1.60
Coordinates	X	5.67	7.83	3.66	-5.12	6.44	6.64
	Y	2.86	4.94	-1.50	-1.44	0.38	0.34
	Z	0.92	1.10	4.67	1.82	-0.72	3.15
		[c]o--------->		[d]o	o	o	o

[a]HBA = hydrogen bond acceptor, [b]HYD = hydrophobic, [c]o-----> = pharmacophore vector

[d]o = pharmacophore point

DMD Fast Forward. Published on September 22, 2006 as DOI: 10.1124/dmd.106.012351
This article has not been copyedited and formatted. The final version may differ from this version.

Table 4. Model statistics for the Inhibitor pharmacophore 2 model and average results after scrambling 10 times.

	Correlation	Total cost (model)	Total cost (fixed)	Total cost (null)
Inhibitor Pharmacophore 2	0.87	151.8	130.7	198.8
Scrambling average	0.56	186.3	127.2	198.8

DMD Fast Forward. Published on September 22, 2006 as DOI: 10.1124/dmd.106.012351
This article has not been copyedited and formatted. The final version may differ from this version.

Table 5. Comprehensive database statistics generated after searching the P-gp database with three pharmacophore models.

Model and search type	Enrichment (E)	Yield (Y%)	Coverage (A%)	GH-Score
Inhibitor model 1 fast	1.4	78	27	0.59
Inhibitor model 1 best	1.3	74	30	0.55
Inhibitor model 2 fast	1.31	72	30	0.53
Inhibitor model 2 best	1.32	73	45	0.53
Substrate model fast	1.8	100	7	0.77
Substrate model best	1.6	90	9	0.69

DMD Fast Forward. Published on September 22, 2006 as DOI: 10.1124/dmd.106.012351
This article has not been copyedited and formatted. The final version may differ from this version.

Table 6. Average molecular properties of each Venn Diagram section (a – e) for the SCUT database search.

Venn diagram section	Average number of hydrogen bond donors	Average number of hydrogen bond acceptors	Average molecular weight	Average rotatable bond number
a.	4.2	13.7	581.6	12.0
b.	2.1	14.7	553.0	8.3
c.	2.7	16.1	655.7	10.9
d.	10.0	37.0	929.5	8.3
e.	5.0	35.0	1201.8	15.0

Table 7. Predicted and empirical physicochemical properties of molecules tested *in vitro*.

Name	Molecular weight	cLogP[a]	Solubility	Bioavailability
Acitretin	326.4	4.84	223.32nM	59%
Cholecalciferol	384.6	6.83	Insoluble	60%
Miconazole	416.1	6.02	28.88mM	25-30%
Misoprostol	382.5	3.37	4.2mM	>80%
Nafcillin	414.5	3.37	Soluble	50%
Repaglinide	452.6	5.80	Insoluble	56 ± 7 %
Salmeterol	415.6	5.02	Slightly soluble	Undetected
Telmisartan	514.6	7.25	Insoluble	43-50 %
Phenelzine	136.2	0.77	124.2mM	NA
Zonisamide	212.2	0.87	3.42mM	NA

[a]cLogP values were retrieved from DrugBank (Wishart et al., 2006).

Figure 1a

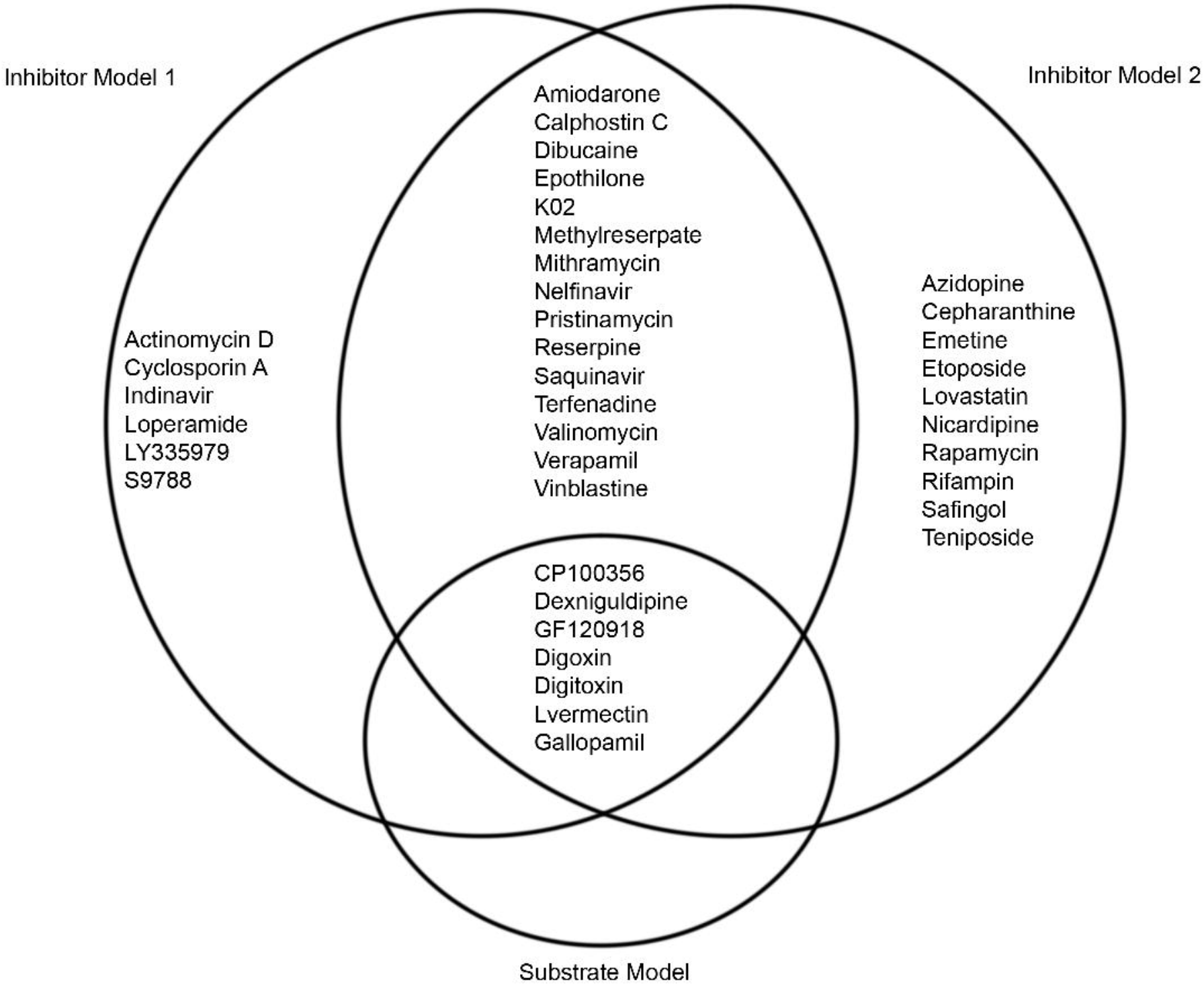
Inhibitor Model 1
Inhibitor Model 2
Substrate Model
Actinomycin D
Cyclosporin A
Indinavir
Loperamide
LY335979
S9788
Amiodarone
Calphostin C
Dibucaine
Epothilone
K02
Methylreserpate
Mithramycin
Nelfinavir
Pristinamycin
Reserpine
Saquinavir
Terfenadine
Valinomycin
Verapamil
Vinblastine
Azidopine
Cepharanthine
Emetine
Etoposide
Lovastatin
Nicardipine
Rapamycin
Rifampin
Safingol
Teniposide
CP100356
Dexniguldipine
GF120918
Digoxin
Digitoxin
Lvermectin
Gallopamil

Figure 1b

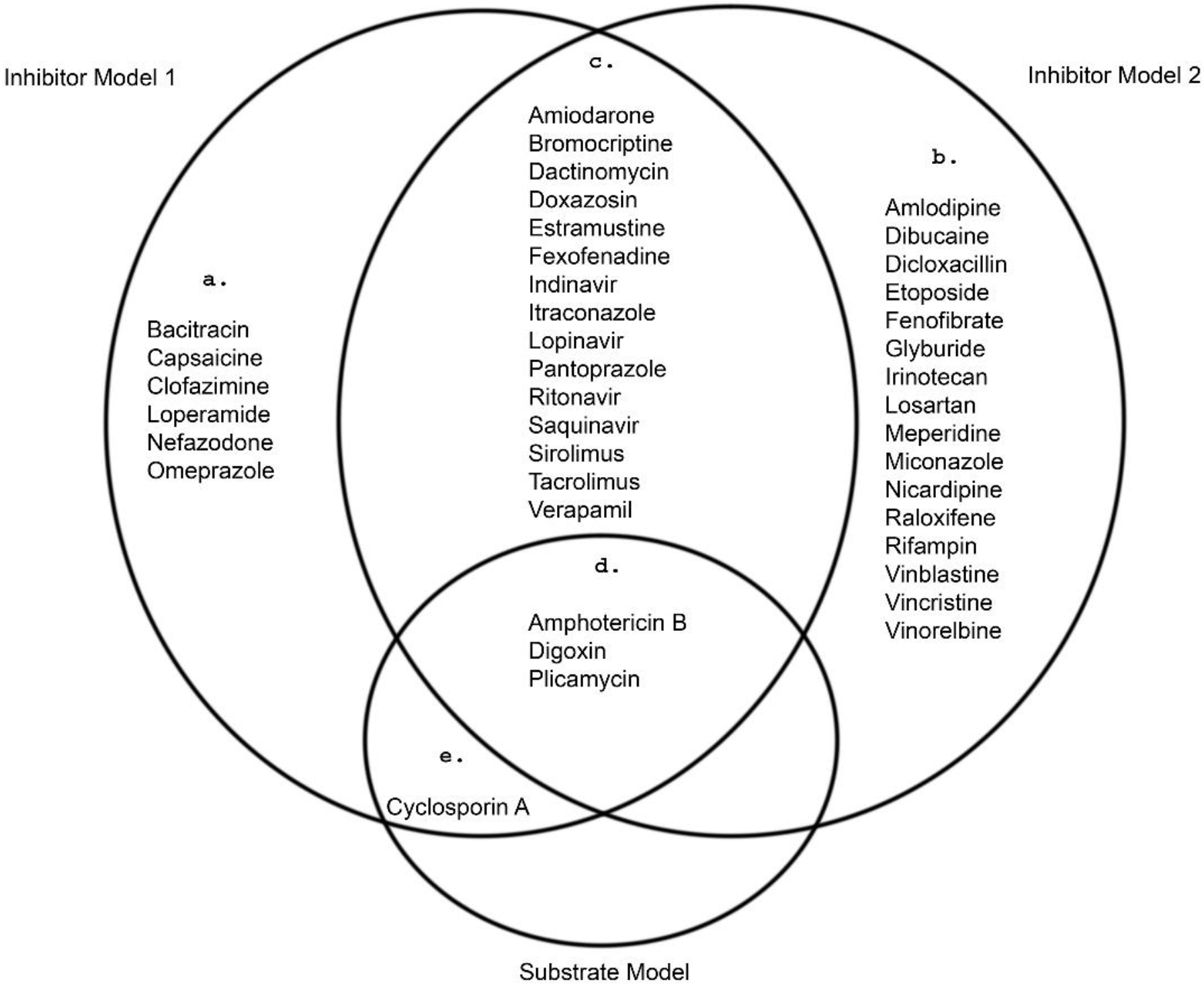
Inhibitor Model 1
Inhibitor Model 2
Substrate Model
a.
Bacitracin
Capsaicine
Clofazimine
Loperamide
Nefazodone
Omeprazole
c.
Amiodarone
Bromocriptine
Dactinomycin
Doxazosin
Estramustine
Fexofenadine
Indinavir
Itraconazole
Lopinavir
Pantoprazole
Ritonavir
Saquinavir
Sirolimus
Tacrolimus
Verapamil
b.
Amlodipine
Dibucaine
Dicloxacillin
Etoposide
Fenofibrate
Glyburide
Irinotecan
Losartan
Meperidine
Miconazole
Nicardipine
Raloxifene
Rifampin
Vinblastine
Vincristine
Vinorelbine
d.
Amphotericin B
Digoxin
Plicamycin
e.
Cyclosporin A

Figure 2

a

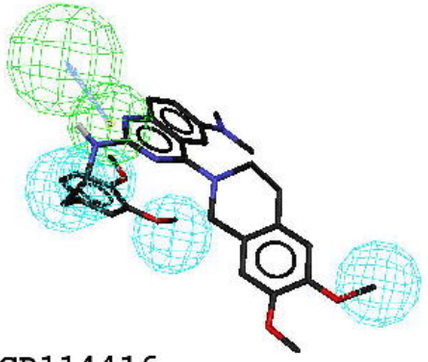

CP114416

b

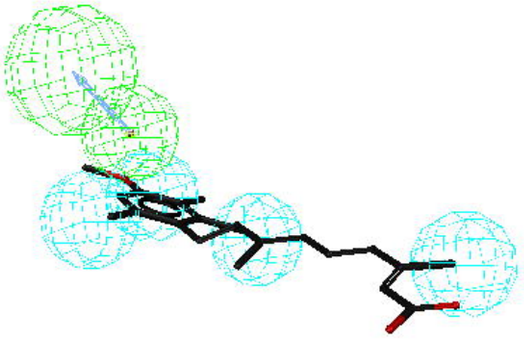

acitretin

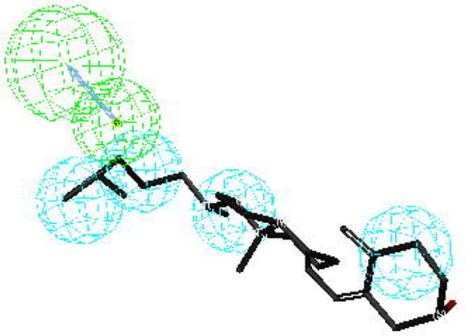

cholecalciferol

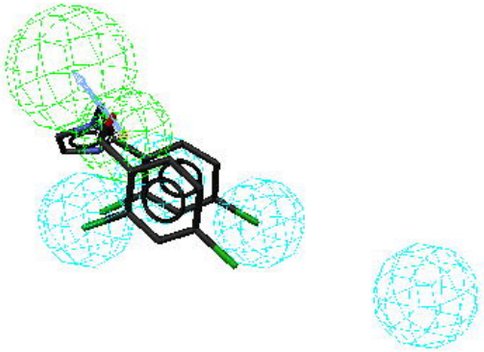

miconazole

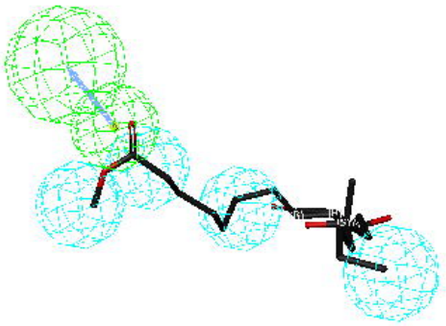

misoprostol

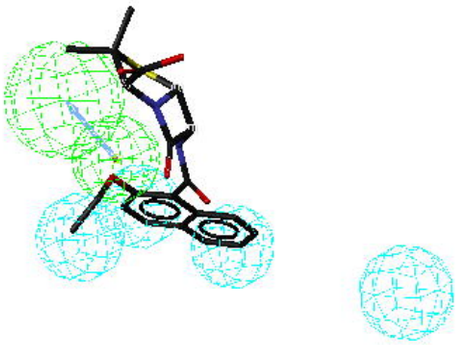

nafcillin

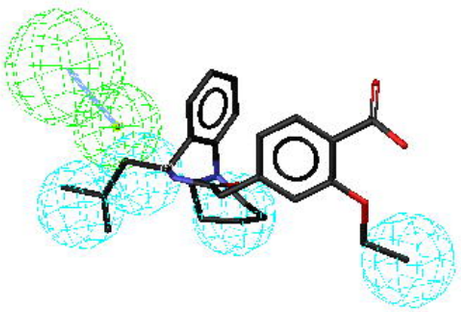

repaglinide

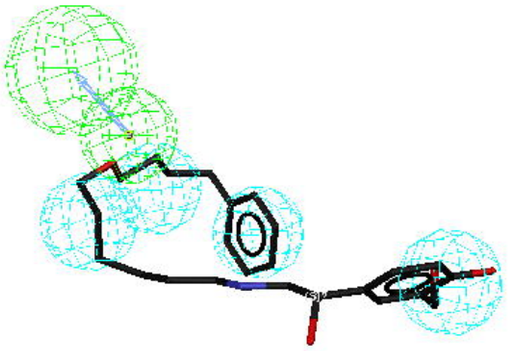

salmeterol

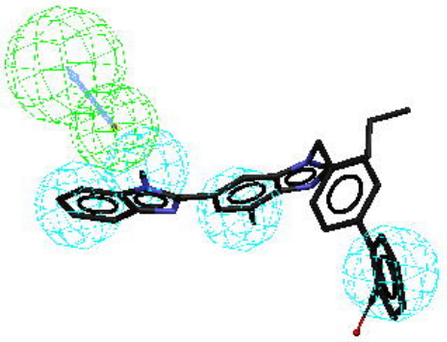

telmisartan

Figure 3

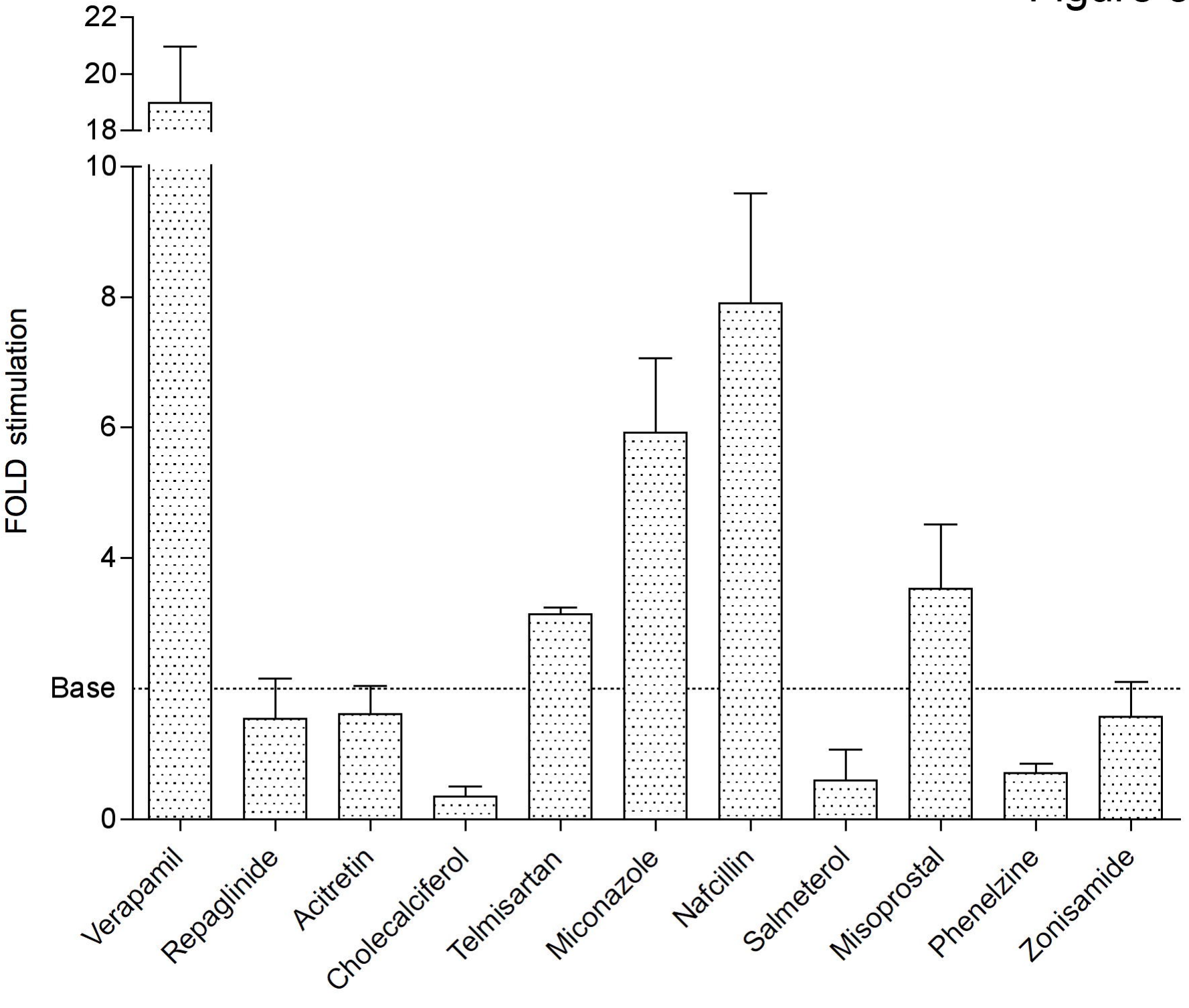
22
20
18
10
8
6
4
Base
0
FOLD stimulation
Verapamil
Repaglinide
Acitretin
Cholecalciferol
Telmisartan
Miconazole
Nafcillin
Salmeterol
Misoprostal
Phenelzine
Zonisamide